RESEARCH ARTICLE

3D visualization of cellular location and cytotoxic reactions of doxorubicin, a chemotherapeutic agent

Verena Richter, Petra Weber, Michael Wagner, Herbert Schneckenburger*

Authors' Affiliations:

Institute of Applied Research, Aalen University, Beethovenstr. 1, 73430 Aalen, Germany

Authors' e-mails: verena.richter@hs-aalen.de
petra.weber@hs-aalen.de
michael.wagner@hs-aalen.de
herbert.schneckenburger@hs-aalen.de **(*corresponding author)**

Abstract

Previously, we reported on the uptake and interaction of cytotoxic doxorubicin in MCF-7 breast cancer cells grown as standard 2-dimensional cell cultures. Now improved experimental techniques – including axial tomography and Light Sheet Fluorescence Microscopy (LSFM) – permit observation of single cells from any side as well as detection of individual layers in multi-cellular spheroids. Therefore, uptake of doxorubicin in the cell nucleus as well re-localization in the cytoplasm at longer incubation times is well documented. Based on a calcein-AM test, we could prove high cytotoxicity in 3D cell cultures at 48–96h after incubation. Simultaneously, disintegration of cell spheroids and formation of a degradation product became obvious. Fluorescence lifetime imaging microscopy (FLIM) is presently used to distinguish the fluorescence of doxorubicin and its degradation product, and Structured Illumination Microscopy (SIM) is suggested to improve resolution down to about 100 nm.

Keywords: fluorescence microscopy, light sheet, axial tomography, cytostatic drug, 3D cell cultures

1. Introduction

Doxorubicin, an anthracycline antibiotic, has been used as a cytostatic drug in cancer chemotherapy, e.g. breast cancer, bronchial carcinoma and lymphoma, for several decades.[1,2] The drug is taken up by cells due to passive diffusion through their membrane and finally intercalates in DNA strands, where it causes chromatin condensation and initiates apoptosis.[3] Due to its fluorescence properties [4] doxorubicin has been localized within the cells, e.g. by wide-field microscopy, hyperspectral imaging [5] and fluorescence lifetime imaging.[6-9] In particular, the latter methods give additional information on intermolecular interactions of doxorubicin with its microenvironment.

While a previous paper was focused on the uptake and intracellular distribution of

doxorubicin in 2-dimensional cell cultures (monolayers) as a function of cholesterol content,[9] we now report on measurements of cellular location and cytotoxicity in more physiological 3D cultures with some emphasis on advanced methods of axial tomography [10,11] and Light Sheet Fluorescence Microscopy (LSFM).[12] Samples range from single cells up to multi-cellular spheroids growing in an agarose gel after incubation with doxorubicin up to 96h.

2. Materials and Methods

MCF-7 human breast cancer cells were obtained from Cell Lines Service (CLS No. 00273, Eppelheim, Germany). Cells were routinely grown in DMEM/HAM F-12 medium supplemented with 10 % fetal calf serum and antibiotics at 37°C and 5 % CO_2. HeLa cervical carcinoma cells (kindly provided by Brigitte Angres, Cellendes GmbH, Reutlingen, Germany) were grown at 37°C, 5% CO_2, in Minimum Essential Medium (MEM) supplemented with 10% FBS, non-essential amino acids, 100 U/mL penicillin, 100 ng/mL streptomycin and 2 mM glutamine. A 1:1 mixture of cell suspension and agarose (1 %) was seeded in agarose-coated cavities of a 24-well culture plate, resulting in 30,000 cells/cavity within a solid matrix. Multicellular spheroids (MCTS) of MCF-7 cells were grown for 7–9 days up to a diameter of about 50 µm after seeding. Single HeLa cells (30,000 cells/cavity) were kept in agarose for 1–2 days prior to measurements. The antitumor antibiotic doxorubicin hydrochloride (Sigma-Aldrich, München, Germany) was prepared as a 2 mM stock solution in ethanol. Individual cavities with single HeLa cells were incubated with doxorubicin in culture medium at a concentration of 4 µM for 2h or 24h. The MCTS of MCF-7 cells were incubated with doxorubicin [6 µM] for variable times between 24h and 96h. In some cases calcein acetomethyl ester (calcein-AM) was also added at a concentration of 5 µM for 30 minutes to check cell viability, since after uptake and cleaving of the ester group, free calcein remains located in viable cells, but is released from deficient cells.[13]

Agarose containing single cells or cell spheroids was taken up by plunging either a cylindrical fluoroethylene propylene capillary (FEP, 380 µm inner diameter, Zeus, Ireland) [14] or a rectangular glass capillary (600µm inner diameter, VitroCom, USA) repeatedly into the solid matrix, so that a column of 30-40 mm was obtained. The advantage of FEP is its refractive index n = 1.33–1.35 which fits the refractive indices of the sample and of water, ensuring optimum imaging conditions with a water immersion lens independent of the sample geometry. Glass capillaries were used, when illumination was perpendicular to the plane surface of the capillary. For fluorescence imaging, an inverted microscope (Axiovert 200M, Carl Zeiss Microimaging GmbH, Germany) was used with various add-on modules for axial rotation, Light Sheet Fluorescence Microscopy and Confocal Laser Scanning Microscopy (laser scanning head Pascal 5, Carl Zeiss Jena). The methods of Light Sheet Microscopy (of cell spheroids) and axial rotation (of single cells) are also depicted schematically in Figure 1. For rotation experiments we used a 63×/0.90 water immersion objective lens in

combination with a FEP capillary fixed in a sample holder on the microscope positioning stage as described earlier.[11] Rotation of the FEP capillaries was performed by a computerised stepping motor with micro-step positioning control (Nema 8 - ST2018S0604-A, SMC11, Nanotec Electronic GmbH & Co.KG, Germany) and an angular resolution of 0.45°. In the present manuscript, only rotations of multiples of 45° are reported. Illumination in Confocal Laser Scanning Microscopy (CLSM) occurred at 488 nm, and fluorescence was registered at $\lambda \geq 560$ nm. Image stacks were recorded at intervals $\Delta z = 1$ µm, and 3D projections for single-sided measurements as well as z projections for various detection angles were calculated using ImageJ.[15]

For Light Sheet Fluorescence Microscopy of cell spheroids embedded in agarose we illuminated the plane surface of a glass capillary by a photonic crystal fibre laser (NKT Photonics SuperK EXTREME with SuperK VARIA tunable single line filter) at $\lambda = 470$ nm (bandwidth: $\Delta\lambda = 10$ nm) used in combination with a single mode fibre (Thorlabs, P1-460B-FC-5). The light sheet was generated by an achromatic cylindrical lens with a numerical aperture $A_N = 0.08$ permitting a beam waist $d = \lambda/A_N \approx 6$ µm and a depth of focus $L = n\lambda/A_N^2 \approx 100$ nm when a refractive index $n = 1.35$ was assumed. The light sheet module was attached to the inverted microscope as reported in Ref. 12, and fluorescence images were recorded by a CCD camera (Zeiss AxioCam MRc) using a long pass filter for $\lambda \geq 515$ nm (permitting detection of doxorubicin, its degradation product as well as calcein) and a 40x/0.75 objective lens.

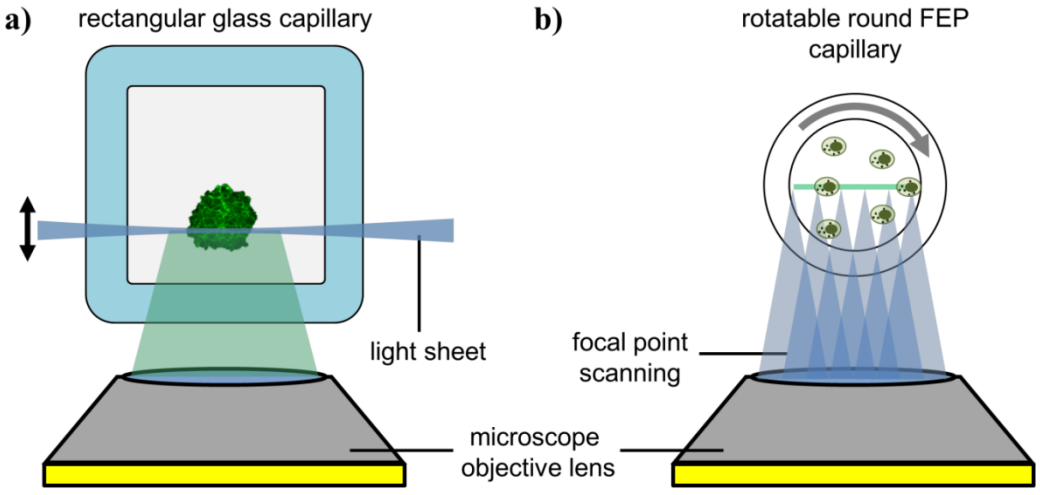

Figure 1. Schemes of Light Sheet Fluorescence Microscopy (LSFM) of cell spheroids (a) and Confocal Laser Scanning Microscopy (CLSM) with axial rotation of individual cells (b; for details see Refs. 10, 11 and 12).

3. Results

Figure 2 shows CLSM transmission (a) and fluorescence (b,c) images of 2 HeLa cells incubated for 2 hours with doxorubicin at various angles of observation. Fluorescence is located in the cell nucleus, and separation of the 2 nuclei depends on the observation angle. While in Fig. 2b views at different angles were calculated from one z stack recorded at 0°,[15] images in Fig. 2c were measured directly at all those angles. A clear enhancement of image quality results in Fig. 2c for all angles except 0°.

Up to 6 hours after application, doxorubicin fluorescence originated from the cell nuclei and – dependent on the angle of detection – gave some information on nuclear architecture. At longer incubation times (see Figure 3 for 24h) a re-localization outside the nuclei occurred, and accumulation in small organelles embedded in the cytoplasm, e.g. lysosomes or endosomes, was observed. Again, axial rotation proved to be helpful for visualization.

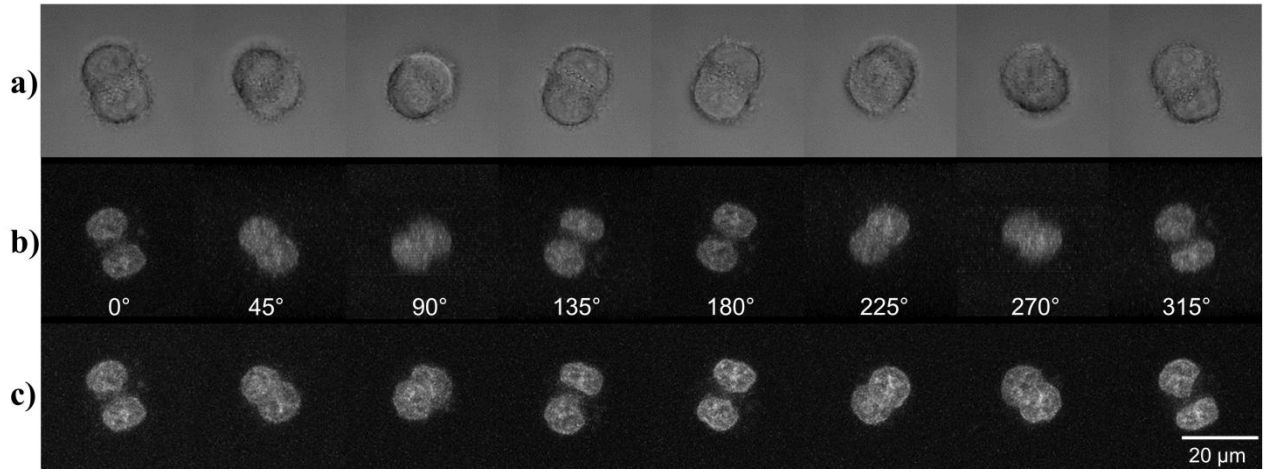

Figure 2. Individual HeLa cells incubated with doxorubicin (4µM, 2h) under variable angles of detection: a) transillumination, b) calculated views from a z stack recorded in one direction (0°), c) z projections calculated from stacks recorded under variable angles (CLSM, excitation wavelength: λ_{ex} = 488 nm; detection range: $\lambda_d \geq$ 560 nm, objective lens: 63×/0.90 water, intervals Δz = 1.0 µm).

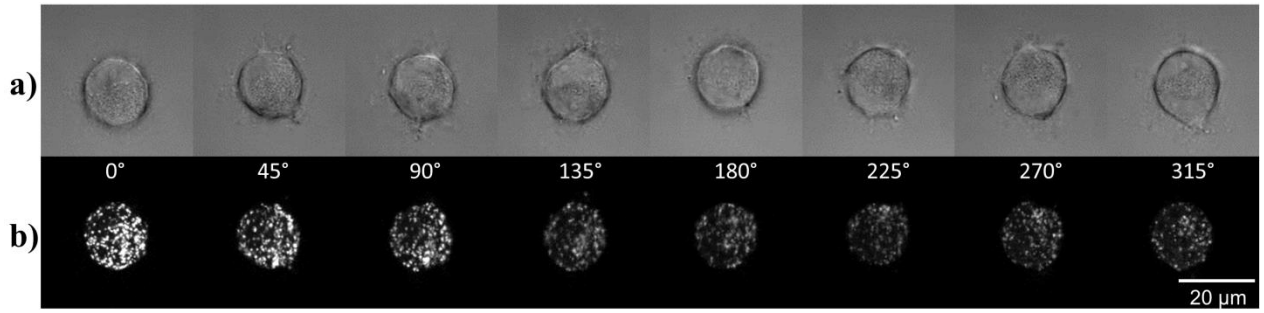

Figure 3. Individual HeLa Cell incubated with doxorubicin (4µM, 24h) under variable angles of detection: a) transillumination, b) z projections calculated from stacks recorded under variable angles (CLSM, excitation wavelength: λ_{ex} = 488 nm; detection range: $\lambda_d \geq$ 560 nm, objective lens: 63×/0.90 water, intervals Δz = 1.0 µm).

Accumulation of doxorubicin in multi-cellular spheroids is documented in Figure 4 (a) for various times after application. Light sheet fluorescence microscopy (LSFM) permits to detect individual cell layers, which otherwise would be superposed by diffuse out-of-focus fluorescence. Figure 4a proves (1) the uptake of doxorubicin in individual cells within 24h, (2) uptake of doxorubicin in almost all cells within 48h, and (3) distribution of doxorubicin over all cells with beginning disintegration of the cell assembly at 72h which continued at 96h. At times above 72 hours diffuse green fluorescence became obvious which may be related to a degradation product.[16] In case of additional incubation with calcein-AM (Figure 4b), fluorescence was dominated by strong green calcein fluorescence at 24h indicating that cells were viable. However, at 48h, as well as at 72h and 96h post application, calcein fluorescence decreased considerably and superimposing red doxorubicin fluorescence became visible (consider the increase of laser irradiance by a factor 7 between 24h and 72h). Probably, severe damage of the cells occurred during this period.

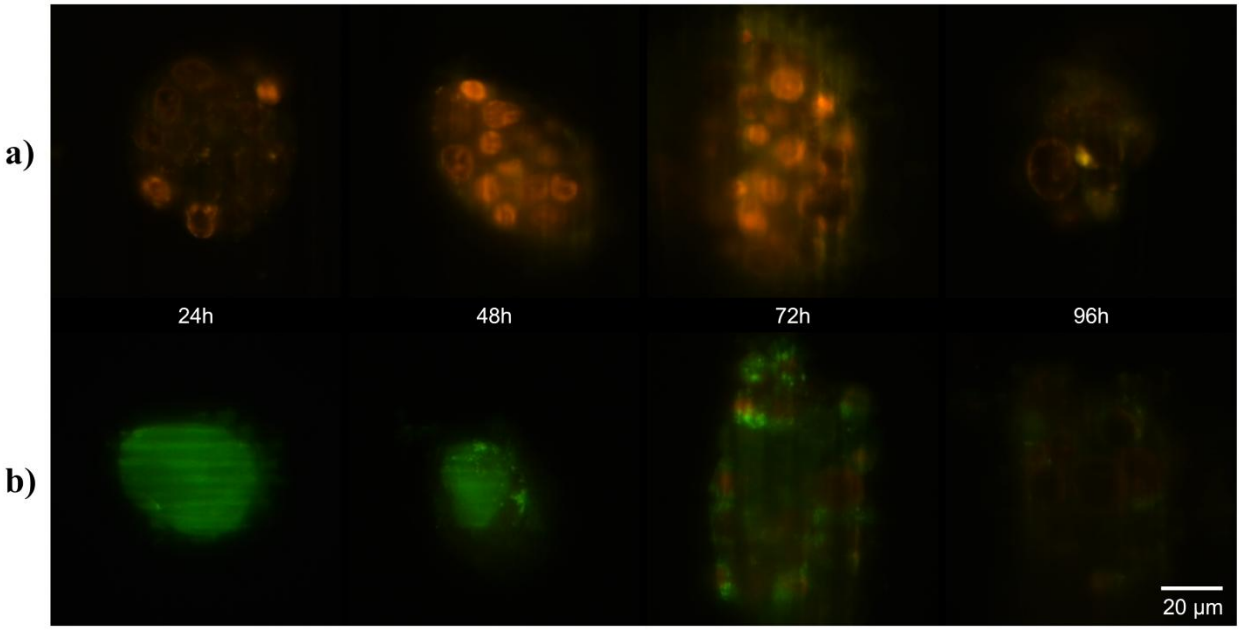

Figure 4. Single layers of spheroids of MCF-7 breast cancer cells in agarose incubated with doxorubicin (6µM, 24h to 96h) without (a) or with (b) additional incubation by calcein-AM (5µM, 30min). While in (a) laser irradiance was kept constant at 800 mW/cm², it was increased in (b) from 115 mW/cm^2 at 24h to 460 mW/cm^2 at 48h and 800 mW/cm^2 at 72h/96h (LSFM, excitation wavelength: λ_{ex} = 470 nm; detection range: $\lambda_d \geq 515$ nm, objective lens: 40×/0.75, exposure time: 4s each).

In cases without additional incubation with calcein-AM, the fluorescence of doxo-rubicin and its degradation product could be well distinguished by fluorescence spectra and lifetimes. This is documented in Figure 5, where fluorescence intensity and lifetime images of doxorubicin are com-pared at 96h after incubation. Intensity

images show an overlap of red doxorubicin fluorescence from the cell nucleus and diffuse green-yellow fluorescence of the degradation product distributed all over the spheroid, whereas lifetime images show a clear distinction of short-lived fluorescence ($\tau \approx 1.8$ ns) of doxorubicin superimposed by longer-lived fluorescence ($\tau \approx 3.5$ ns) of its degradation product. This proves that in addition to fluorescence spectroscopy nano-second fluorescence lifetime imaging (further reported in Ref. 9) is a valuable method for identifying various molecular species.

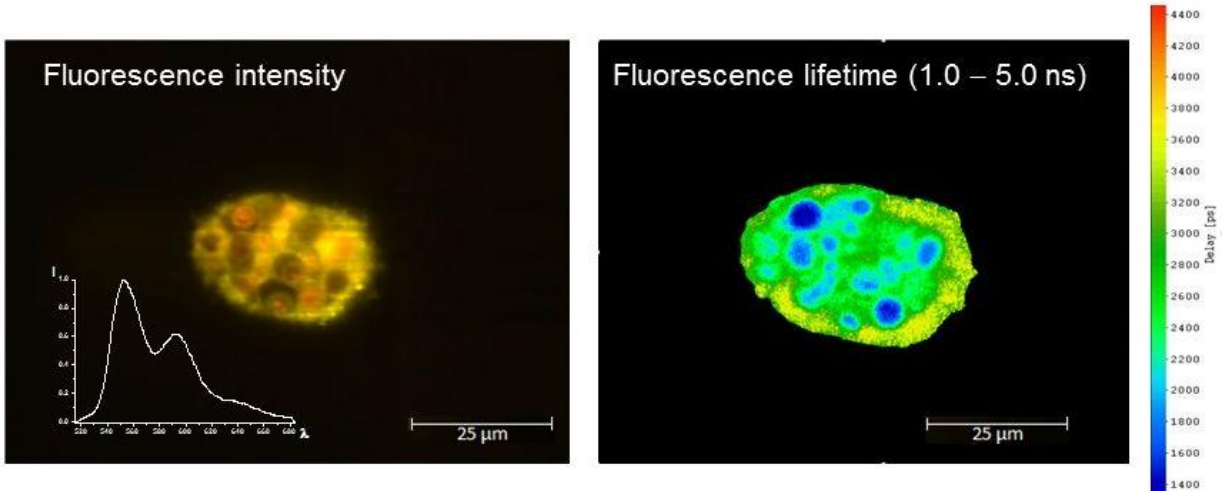

Figure 5. Fluorescence intensity and spectrum (left) as well as fluorescence lifetime (right) of a MCF-7 cell spheroid incubated for 96h with doxorubicin (6 µM) including a lifetime scale in picoseconds (excitation wavelength: $\lambda_{ex} = 470$ nm; detection range: $\lambda_d \geq 515$ nm).

Discussion

Doxorubicin has the unique advantage that due to its red autofluorescence it can be easily localized in living cells or tissues. This advantage has been used by various authors to measure its binding to nano-particles or other carrier systems and to apply these particles to living cells. Only a few measurements of cellular uptake and distribution of free doxorubicin have been reported in the literature. They are in some cases related to spectral imaging [17] or fluorescence lifetime imaging microscopy (FLIM),[18,19] since spectral bands or fluorescence lifetimes often reflect the interaction of a fluorescent dye with its molecular or cellular environment. In the present manuscript, we used the FLIM technique for another application: to distinguish between doxorubicin and its degradation product.

A general problem of 3D microscopy is – besides scattering and limited light penetration into the sample – a low depth of focus, which is considerably smaller than the size of the specimen. Therefore, an image from the focal plane is often superposed by out-of-focus images giving altogether rather poor information of the sample. This problem can be overcome by confocal or multi-photon laser scanning microscopy [19] as well as by Light Sheet Fluorescence Microscopy (LSFM).[20,21] In comparison with previous studies [21], LSFM

was now applied over a prolonged incubation period of doxorubicin (24–96h) and combined with some visualization of cytotoxicity. This allowed us to obtain more detailed information: uptake of doxorubicin occurred within almost all cells of a multi-cellular MCF-7 spheroid within 48h, and cytotoxic reactions occurred between 48h and 96h. In addition, axial tomography of single cells proved some exclusion of doxorubicin from the cell nucleus and re-distribution in the cytoplasm, however, the impact of this re-distribution on cytotoxicity remains unclear, so far. Super-resolution microscopy, e.g. Structured Illumination Microscopy (SIM) with a resolution down to 100 nm, may give further information on sub-cellular architecture and cytotoxic reactions of doxorubicin (unpublished result).

Conclusion

We conclude that methods of 3D microscopy (Light Sheet Fluorescence Microscopy or CLSM in combination with axial rotation) are valuable tools for visualizing a chemotherapeutic agent and its reactions in single cells and larger cell assemblies. Spectral imaging or fluorescence lifetime imaging microscopy (FLIM) may support identification of involved molecular species. Doxorubicin uptake occurred within almost all cells of a multi-cellular MCF-7 spheroid within 48h, and cytotoxic reactions were observed between 48h and 96h. CLSM in combination with axial tomography permits detection of doxorubicin and its interactions with sub-cellular resolution, and methods of super-resolution microscopy, e.g. Structured Illumination Microscopy (SIM), may further improve this resolution.

Acknowledgment

This project was funded by the Ministerium für Wissenschaft, Forschung und Kunst Baden-Württemberg as well as by the Bundesministerium für Bildung und Forschung (Projekt VAGeB, FKZ 03FH002PX5). The authors thank Claudia Hintze for the skillful technical assistance.

References

(1) Carter, SK, Blum, RH. New chemotherapeutic agents – Bleomycin and Adriamycin, CA Cancer J. Clin., 1974, 24: 322–331. doi:10.3322/canjclin.24.6.322.

(2) Blum, RH, Carter, SK. Adriamycin. A new anticancer drug with significant clinical activity, Ann. Intern. Med., 1974, 80: 249–259. doi:10.7326/0003-4819-80-2-249.

(3) Li, ZX, Wang, TT, Wu, YT, Xu, CM, Dong, MY, Sheng, JZ, Huang, HF. Adriamycin induces H2AX phosphorylation in human spermatozoa, Asian J. Androl., 2008, 10: 749–757. doi: 10.1111/j.1745-7262.2008.00400.x.

(4) Karukstis, KK, Thompson, EH, Whiles, JA, Rosenfeld, RJ. Deciphering the fluorescence signature of daunomycin and doxorubicin, Biophys. Chem., 1998, 73: 249–263. doi: 10.1016/S0301-4622(98)00150-1.

(5) Haaland, D.M, Jones, HD, van Benthem, MH, Sinclair, MB, Melgaard,

DK, Stork, CL, Pedroso, MC, Liu, P, Brasier, AR, Andrews, NL et al. Hyperspectral confocal fluorescence imaging: Exploring alternative multivariate curve resolution approaches, Appl. Spectrosc., 2009, 63: 271–279. doi:10.1366/000370209787598843.

(6) Chen, NT, Wu, CY, Chung, CY, Hwu, Y, Cheng, SH, Mou, CY, Lo, LW. Probing the dynamics of doxorubicin-DNA intercalation during the initial activation of apoptosis by fluorescence lifetime imaging microscopy (FLIM), PLoS One, 2012, 7: e44947. doi: 10.1371/journal.pone. 0044947.

(7) Bakker, GJ, Andresen, V, Hoffman, RM, Friedl, P. Fluorescence lifetime microscopy of tumor cell invasion, drug delivery, and cytotoxicity, Methods Enzymol., 2012, 504: 109–125. doi:10.1016/B978-0-12-391857-4.00005-7.

(8) Dai, X, Yue, Z, Eccleston, ME, Swartling, J, Slater, NK, Kaminski, CF. Fluorescence intensity and lifetime imaging of free and micellar-encapsulated doxorubicin in living cells, Nanomedicine, 2008, 4: 49–56. doi: 10.1016/j.nano. 2007.12.002.

(9) Weber, P, Wagner, M, Schneckenburger, H. Cholesterol dependent uptake and interaction of doxorubicin in MCF-7 breast cancer cells, Int. J. Mol. Sci., 2013, 14: 8358–8366. doi: 10.3390/ijms14048358.

(10) Bruns, T, Schickinger, S, Schneckenburger, H. Sample holder for axial rotation of specimens in 3D Microscopy, J. Microsc., 2015, 260(1): 30-36. doi: 10.1111/jmi.12263.

(11) Richter, V, Bruns, S, Bruns, T, Weber, P, Wagner, M, Cremer, C, Schneckenburger, H. Axial tomography in live cell laser microscopy, J. Biomed. Opt. 2017, 22(9): 091505. doi: 10.1117/1.JBO.22.9.091505.

(12) Bruns, T, Bauer, M, Bruns, S, Meyer, H, Kubin, D, Schneckenburger, H. Miniaturized modules for light sheet microscopy with low chromatic aberration, J. Microsc., 2016, 264(3): 261-267. doi: 10.1111/jmi.12439.

(13) Bratosin D, Mitrofan L, Palii C, Estaquier J, Montreuil J. Novel fluorescence assay using calcein-AM for the determination of human erythrocyte viability and aging. Cytometry A, 2005, 66(1): 78-84. doi: 10.1002/cyto.a.20152.

(14) Weber, M, Mickoleit, M, Huisken, J. Multilayer mounting for long-term light sheet microscopy of zebrafish, J. Vis. Exp., 2014, 84: e51119. doi: 10.3791/51119.

(15) Rasband, WS. ImageJ, U. S. National Institutes of Health, Bethesda, Maryland, USA, http://imagej.nih.gov/ij/, 1997-2016.

(16) Hovorka, O, Šubr, V, Vetvicka, D, Kovar, L., Strohalm, J, Strohalm, M, Benda, A, Hof, M, Ulbrich, K, Rihova, B. Spectral analysis of doxorubicin accumulation and the indirect quantification of its DNA intercalation, Eur. Journal of Pharmaceutics and Biopharmaceutics 2010, 76(3): 514–524. doi: 10.1016/j.ejpb.2010. 07.008.

(17) Mohapatra S, Nandi S, Chowdhury R, Das G, Ghosh S, Bhattacharyya K. Spectral mapping of 3D multi-cellular tumor spheroids: time-resolved confocal microscopy, Phys. Chem. Chem. Phys., 2016, 18(27): 18381-18390. doi: 10.1039/ c6cp02748b.

(18) Bakker, GJ, Andresen, V, Hoffman, RM, Friedl P. Fluorescence lifetime microscopy of tumor cell invasion, drug delivery, and cytotoxicity, Methods Enzymol., 2012, 504: 109-125. doi:10.1016/B978-0-12-391857-4.00005-7.

(19) Carlson M, Watson AL, Anderson L, Largaespada DA, Provenzano PP. Multiphoton fluorescence lifetime imaging of chemotherapy distribution in solid tumors, J Biomed Opt., 2017, 22(11): 1-9. doi: 10.1117/1.JBO.22.11.116010.

(20) Fei, P, Lee, J, Packard, RR, Sereti, KI, Xu, H, Ma J, Ding, Kang, Chen, H, Sung, K, Kulkarni, R, Ardehali, R, Kuo, CC, Xu, X, Ho, CM, Hsiai, TK. Cardiac Light-Sheet Fluorescent Microscopy for Multi-Scale and Rapid Imaging of Architecture and Function, Sci Rep., 2016, 6: 22489. doi: 10.1038/srep22489.

(21) Bruns, T, Schickinger, S, Schneckenburger, H. Single plane illumination module and micro-capillary approach for a wide-field microscope, J Vis Exp., 2014, 90: e51993. doi: 10.3791/51993.

